Light-Driven MOF Micromotors for Efficient Gold Recovery from Aqueous Solutions

Leena Alqmize, Yanhan Wang , Prof. Kang Liang

l.alqmize@student.unsw.edu.au, Yanhan.wang@student.unsw.edu.au, Kang.liang@unsw.edu.au

Abstract

The increasing demand for clean water and the extraction of raw materials has motivated the development of technologies combining water purification with resource recovery. Gold contained in industrial wastewaters and leachates of electronic waste poses a problem but is at the same time a resource. Traditional extraction methods often involve hazardous reagents, complex processing steps, and substantial chemical or energy consumption, highlighting the need for more sustainable alternatives. This project investigates a MOF-on-MOF platform for light-driven gold recovery from aqueous solutions by combining the structural stability of UIO-66 with the photoactive properties of the porphyrinic metal–organic frameworks MOF-525 and MOF-545. UIO-66@MOF-525 and UIO-66@MOF-545 composite materials are synthesized, and their structural and morphological characteristics are investigated to evaluate the formation and functionality of the heterostructures. The efficiency of these materials in recovering gold in light Irradiation or under photocatalytic condition will be evaluated to understand the benefits of creating a multi-MOF composite. Combining adsorption and photocatalysis into one process, this research seeks to produce an effective method for resource extraction with a positive environmental impact.

Date: August 24, 2026

Code: https://github.com/kaust-academy/your-project

Project Page: https://your-project-page.github.io

Contents

1 Introduction **2**

1.1 Background . . . 2

1.2 Metal–Organic Frameworks for Sustainable Gold Recovery . . . 2

2 Related Work **2**

3 Methodology **3**

3.1 Experimental Design . . . 3

3.2 Synthesis of UIO-66 . . . 3

3.3 Synthesis of MOF-525 . . . 3

3.4 Synthesis of MOF-545 . . . 4

3.5 Formation of UIO-66@MOF-525 . . . 4

3.6 Formation of UIO-66@MOF-545 . . . 4

3.7 Characterization of the Synthesized Materials . . . 4

3.8 Gold-Recovery Experiments . . . 4

4 Results **5**

4.1 Structural and Morphological Characterization . . . 5

4.2 XRD of UIO-66@MOF-545 . . . 7

4.3 UV–Vis Analysis of Gold Recovery . . . 7

5 Discussion **9**

6 Limitations and Future Work **10**

7 Conclusion **10**

8 Acknowledgments **11**

9 References **11**

1 Introduction

1.1 Background

With the growing demand for clean water and natural resources, sustainable water management has become an increasingly important challenge on a global scale. Water sustainability involves not only ensuring access to clean water but also recovering valuable resources from wastewater through processes that minimize environmental impact. The recovery of metals from aqueous systems may reduce the amount of waste and increase the efficiency of resource use and aid in the implementation of a circular economy [**1**, **2**, **3**].

Gold is one of the most valuable metals that can be found in industrial wastewater and in electronic waste leachates. As gold is widely used in various electronic devices, as well as in catalysis and other high-tech applications, Recovering gold from these aqueous waste streams can therefore provide both economic and environmental benefits [**4**]. Conventional approaches for gold extraction and recovery include cyanide-based processes and solvent extraction; however, these methods may involve hazardous chemicals, complex processing steps, and considerable chemical or energy consumption [**4**, **5**]. Developing alternative approaches capable of recovering gold efficiently under milder and more environmentally sustainable conditions is highly desirable [**5**].

1.2 Metal–Organic Frameworks for Sustainable Gold Recovery

Metal–organic frameworks (MOFs) have attracted significant attention because of their high surface area, tunable pore structures, and versatile chemical properties, making them suitable for a wide range of environmental applications [**5**, **6**]. UIO-66 is particularly well known for its excellent chemical and structural stability, Porphyrinic MOFs such as MOF-525 and MOF-545 contain photoactive porphyrin linkers and porous structures that provide potential advantages for light-assisted adsorption and reduction processes [**7**, **8**]. MOF-on-MOF heterostructures can combine the complementary structural and functional properties of these materials within a single system [**6**].

In this project, UIO-66-based MOF-on-MOF composites are developed by growing MOF- 525 and MOF-545 on UIO-66 particle. The UIO-66@MOF-525 and UIO-66@MOF-545 systems are designed to combine the structural stability of UIO-66 with the light-harvesting and photocatalytic properties of the porphyrinic MOFs [**7**, **8**]. UIO-66 is used as a common core to provide a consistent structural platform for the growth of MOF-525 and MOF-545, allowing the two MOF-on-MOF systems to be compared under similar structural conditions. Their structural and morphological characteristics will be examined, followed by evaluation of their performance for gold recovery from aqueous solutions under light irradiation. This comparison will help determine how the different structures and morphologies of MOF-525 and MOF-545 affect gold recovery performance. By combining adsorption with photocatalytic reduction, this study aims to develop a light-driven MOF- based platform for sustainable gold recovery from aqueous waste streams [**7**, **8**].

2 Related Work

Metal–organic frameworks (MOFs) have been widely investigated for environmental applications because of their high surface area, tunable pore structures, and chemical versatility. Zr-based MOFs are particularly attractive for aqueous applications because of their chemical and structural stability and have shown potential for Au(III) recovery from aqueous solutions [**5**]. Porphyrinic MOFs such as MOF-525 and MOF-545 provide additional functionality through their porphyrin-based

linkers and light-responsive properties. Previous work has shown that porphyrin-based MOFs can enhance Au(III) recovery under light irradiation, supporting their potential for light-assisted gold recovery [7].

Gold recovery from secondary resources, particularly electronic waste, has received considerable attention because of the economic value of gold and the increasing generation of electronic waste [4]. MOFs provide a potential approach for capturing dissolved gold species through interactions with their porous structures and chemical functionalities. Zr-based MOFs have demonstrated selective Au(III) adsorption from aqueous solutions [5]. Light-promoted gold extraction using UIO-based MOFs has also been reported, showing the potential of combining MOF adsorption with light-assisted processes [8].

Light-responsive MOF materials also have potential for integration into nanomotor systems. MOF-525-based nanomotors have been developed for water treatment, combining self-propulsion, contaminant capture, and photocatalytic removal in aqueous systems [9]. Active motion can increase interactions between the material and dissolved species, providing a possible approach for improving mass transfer during water treatment.

MOF-on-MOF materials offer a strategy for combining the properties of different MOFs within a single structure. Previous work has demonstrated controlled growth of MOF-on-MOF heterostructures and shown that the architecture of the resulting material can influence its properties [6]. In this study, UIO-66 is used as a stable core for the growth of MOF-525 and MOF-545. The resulting UIO-66@MOF-525 and UIO-66@MOF-545 materials are investigated for gold recovery under light and dark conditions, providing a foundation for their potential future application in light-driven MOF nanomotors.

3 Methodology

3.1 Experimental Design

The experimental approach was designed to investigate UIO-66-based MOF-on-MOF materials for light-driven gold recovery from aqueous solutions. UIO-66 was first prepared and subsequently used as the core material for the formation of UIO-66@MOF-525 and UIO-66@MOF-545. MOF-525 and MOF-545 were also synthesized separately to provide reference materials for comparison.

The study consisted of material synthesis, washing and activation where applicable, structural and morphological characterization, and gold-recovery testing. The synthesized materials were evaluated under both light and dark conditions to investigate the effect of light irradiation on the gold-recovery process.

3.2 Synthesis of UIO-66

UIO-66 was prepared by dissolving $ZrCl_4$ (233 mg) in 40 mL of DMF using sonication. Terephthalic acid (TA, 166 mg) was then added and the mixture was sonicated. Acetic acid (3 mL) was subsequently added as a modulating agent, followed by another sonication step.

The mixture was transferred to a round-bottom flask and heated in an oil bath at 120 °C for 24 h. After the reaction, the solid product was washed three times with DMF and three times with ethanol. The material was solvent-exchanged by soaking in ethanol for 2 days and then dried under vacuum at 60 °C for 12 h before being used for the MOF-on-MOF synthesis.

3.3 Synthesis of MOF-525

MOF-525 was prepared separately as a reference porphyrinic MOF. $ZrCl_4$ (14 mg) was added to 10 mL of DMF and sonicated. TCPP (10 mg) was then added, followed by sonication. Myristic

acid (2.5 g) was subsequently introduced as the modulating agent and the mixture was sonicated again.

The reaction mixture was placed in an oven at 120 °C for 24 h. The resulting solid was collected and washed three times with DMF and three times with ethanol.

3.4 Synthesis of MOF-545

MOF-545 was prepared using the same general procedure as MOF-525, but with benzoic acid as the modulating agent. $ZrCl_4$ (14 mg) and TCPP (10 mg) were added to 10 mL of DMF, with sonication after each addition. Benzoic acid (1 g) was then added and the mixture was sonicated.

The reaction mixture was heated at 120 °C for 24 h. The resulting solid was collected and washed three times with DMF and three times with ethanol.

3.5 Formation of UIO-66@MOF-525

The UIO-66@MOF-525 heterostructure was prepared by introducing the pre-synthesized UIO-66 into the MOF-525 precursor mixture. UIO-66 (100 mg) was added to 80 mL of DMF, followed by $ZrCl_4$ (50 mg), TCPP (20 mg), and myristic acid (2.5 g). Sonication was carried out after each addition to maintain thorough mixing of the reaction components.

The mixture was heated at 120 °C for 24 h. After synthesis, the resulting material was collected and washed three times with DMF and three times with ethanol.

3.6 Formation of UIO-66@MOF-545

The UIO-66@MOF-545 heterostructure was prepared using a reduced-scale MOF-545 synthesis. UIO-66 (20 mg) was added to 10 mL of DMF, followed by $ZrCl_4$ (10 mg), TCPP (4 mg), and benzoic acid (100 mg). Each component was followed by a sonication step to promote uniform mixing.

The reaction mixture was heated at 120 °C for 24 h. The resulting material was collected and washed three times with DMF and three times with ethanol.

3.7 Characterization of the Synthesized Materials

The synthesized materials were characterized to determine their morphology, elemental composition, and crystalline structure. SEM was used to examine the morphology of the particles and investigate the formation of the porphyrinic MOF on the UIO-66 surface. EDS and elemental mapping were used to analyze the elemental composition and spatial distribution of characteristic elements. XRD was used to identify the crystalline phases and compare the diffraction patterns of the individual MOFs with those of the MOF-on-MOF materials.

3.8 Gold-Recovery Experiments

The gold-recovery experiments were performed using an aqueous $HAuCl_4$ solution with an Au(III) concentration of 25 mg L^{-1}. A $HAuCl_4$ solution without MOF material was used as a control.

For each synthesized material, 2.5 mg of the sample was added to 10 mL Au(III) solution. The samples were first kept in the dark for 30 min to allow adsorption equilibrium to be established. After this dark adsorption period, a UV–Vis measurement was taken and defined as t = 0 for the subsequent irradiation experiment.

After the initial measurement, the samples were divided into light and dark conditions. The samples assigned to the light condition were exposed to light irradiation for 30 min, while the dark samples remained covered for the same period. A second UV–Vis measurement was then taken from all samples.

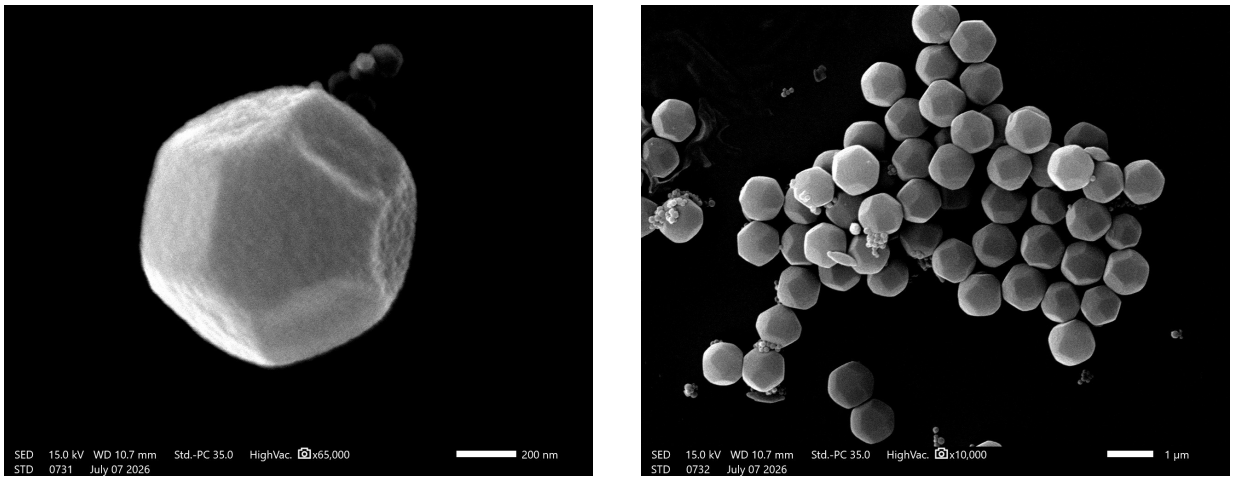
This procedure was performed for UIO-66, MOF-525, MOF-545, UIO-66@MOF-525, and UIO-66@MOF-545. The two UV–Vis measurements were compared to determine the change in the gold-containing solution over the experimental period. The Au(III) control and dark condition were used to distinguish changes associated with the MOF materials and light irradiation.

The comparison between the individual MOFs and MOF-on-MOF materials was used to investigate how the different structures influenced gold recovery and to evaluate the potential of the UIO-66-based heterostructures for light-driven gold recovery from aqueous solutions.

4 Results

4.1 Structural and Morphological Characterization

SEM was used to examine the morphology of the synthesized materials and assess whether the expected structures were obtained before proceeding to the gold-recovery experiments.



(a) MOF-525 particle at higher magnification. **(b)** Lower magnification

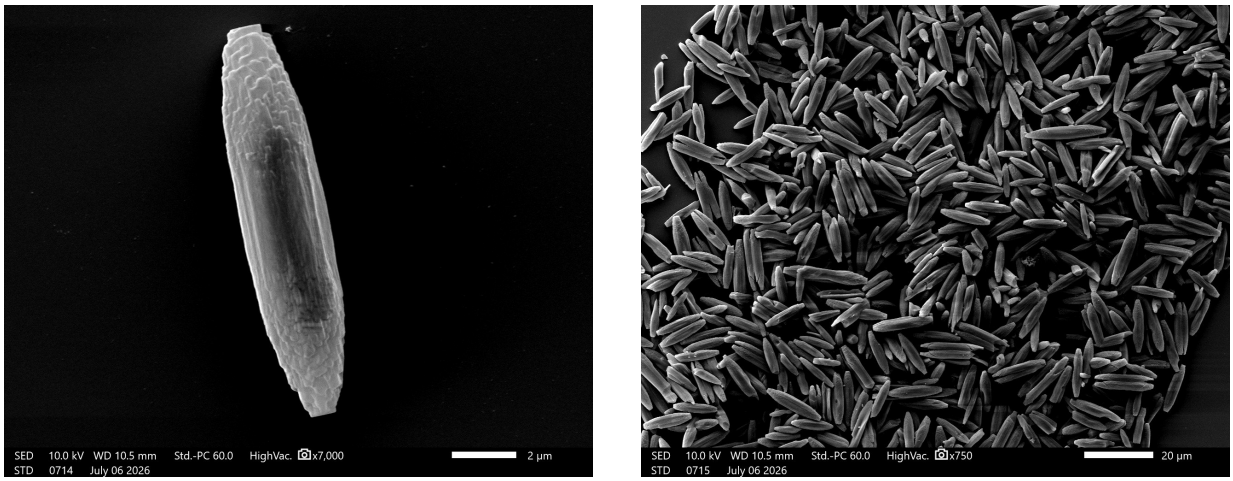
Figure 1 SEM images of MOF-525 at different magnifications.

The morphology of MOF-525 was consistent with the expected structure and was used as a reference for comparison.

The MOF-545 morphology provided a reference for assessing its formation on the UIO-66 surface.

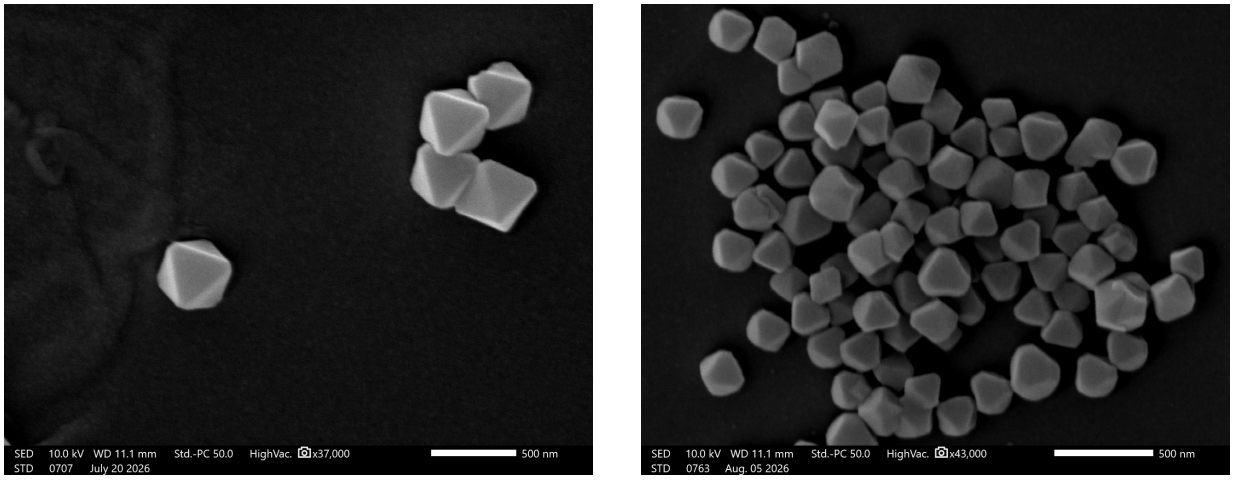
The UIO-66 morphology was used as the reference for evaluating the changes following modification.

The observed surface features were consistent with MOF-545 growth on the UIO-66 particles, with sufficient morphology and uniformity to proceed to the gold-recovery experiments. The UIO-66@MOF-525 synthesis did not produce a sufficiently clean and uniform morphology consistent with the expected MOF-on-MOF structure, so the material was not progressed to the gold-recovery experiments.



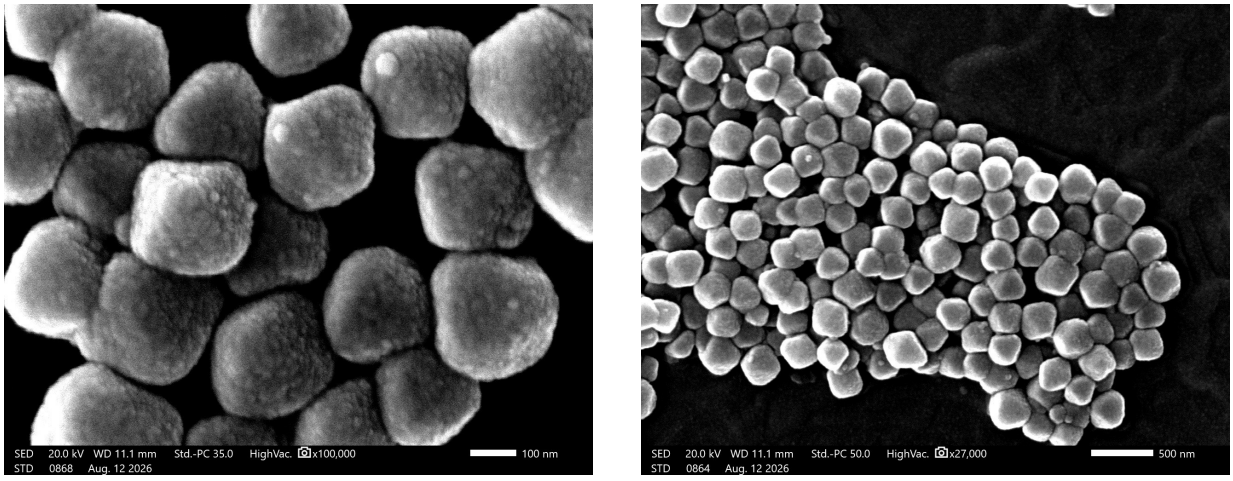
(a) MOF-545 particle at higher magnification. **(b)** Lower magnification

Figure 2 SEM images of MOF-545 at different magnifications.



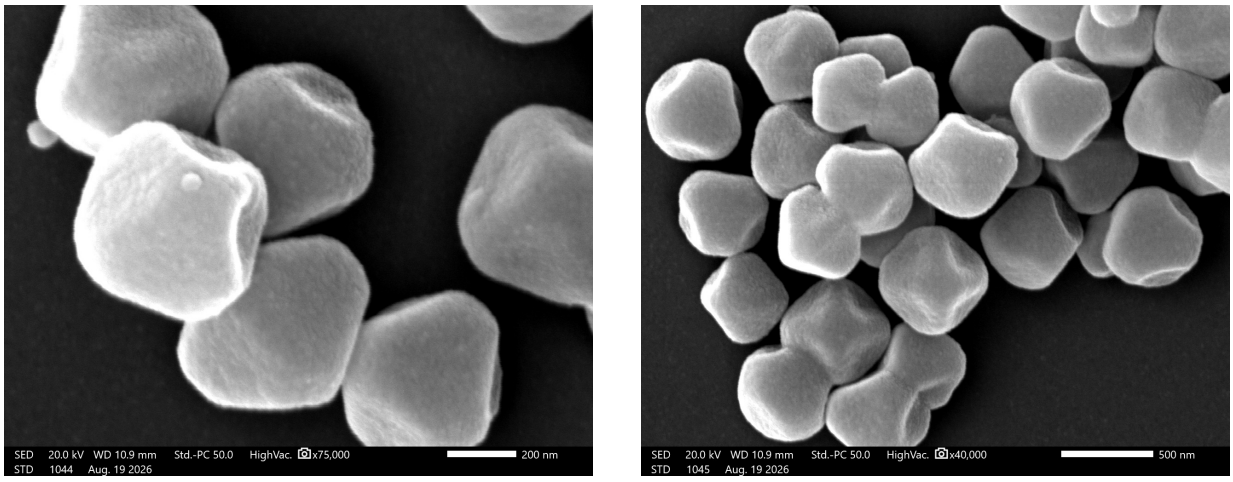
(a) Higher-magnification. **(b)** Lower-magnification .

Figure 3 SEM images of UIO-66 at different magnifications.



(a) Higher-magnification. **(b)** Lower-magnification.

Figure 4 SEM images of UIO-66@MOF-545 at different magnifications.



(a) Higher-magnification image **(b)** Lower-magnification image

Figure 5 SEM images of UIO-66@MOF-525 at different magnifications.

4.2 XRD of UIO-66@MOF-545

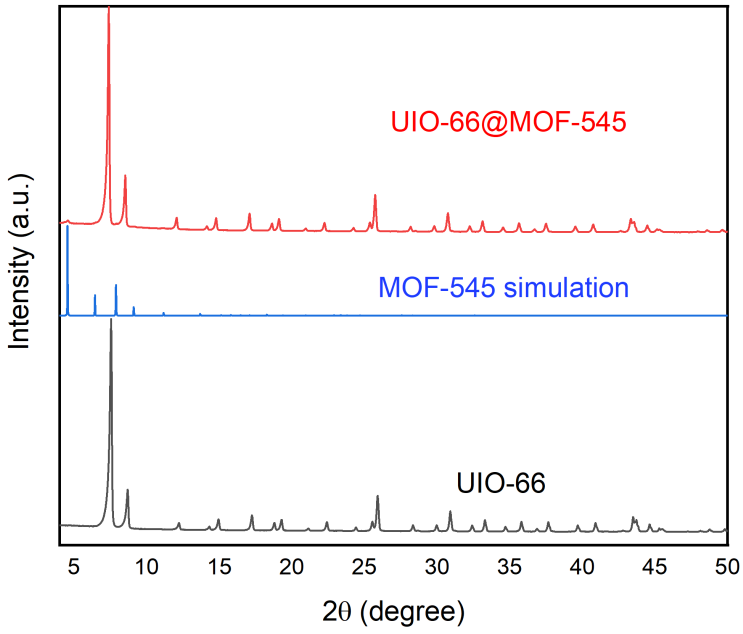
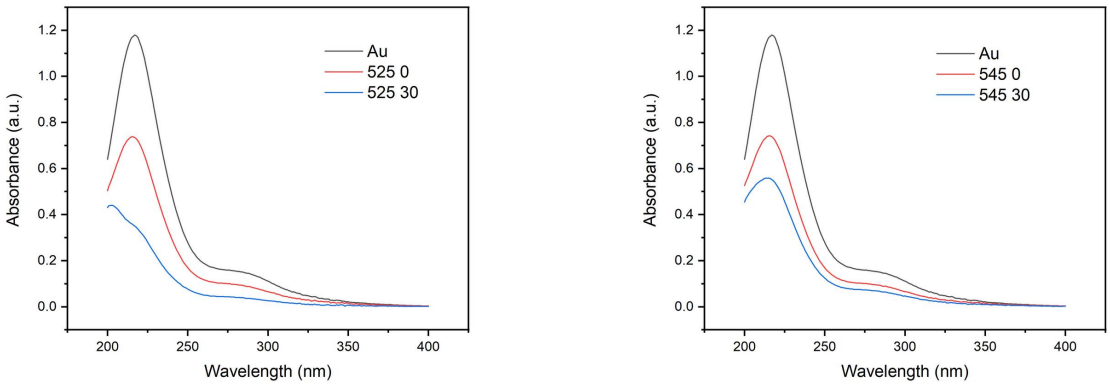


Figure 6 XRD patterns of UIO-66@MOF-545, simulated MOF-545, and UIO-66, showing good peak alignment.

4.3 UV–Vis Analysis of Gold Recovery

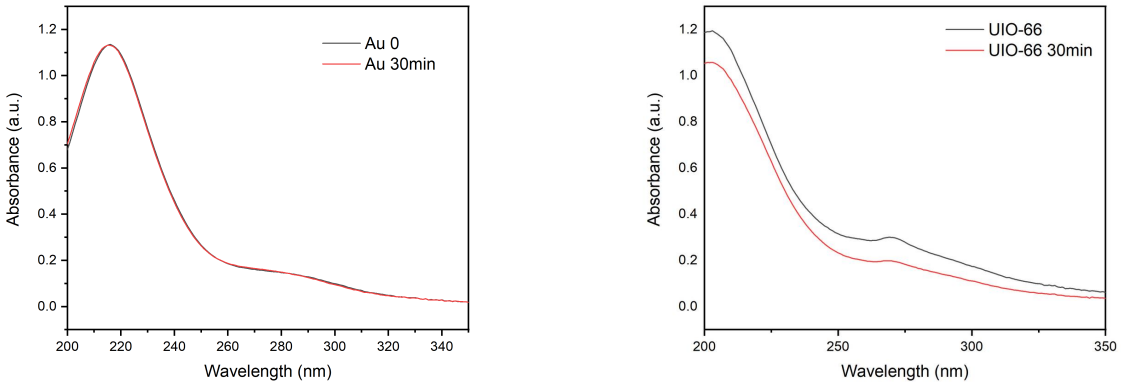
UV–Vis spectroscopy was used to compare the Au(III) concentration before and after treatment with the different MOF materials. The initial measurement was taken after the 30 min dark adsorption period, followed by a second measurement after a further 30 min under the specified conditions. The Au(III)-only sample was used as the control for comparison.



(a) MOF-525 . **(b)** MOF-545.

Figure 7 UV–Vis spectra showing the Au(III) concentration before and after 30 min treatment.

Both MOF-525 and MOF-545 showed a decrease in absorbance after 30 min, indicating a decrease in the remaining Au(III) concentration in solution. MOF-525 showed a gold-removal efficiency of 70.33%, while MOF-545 showed a removal efficiency of 52.6%.

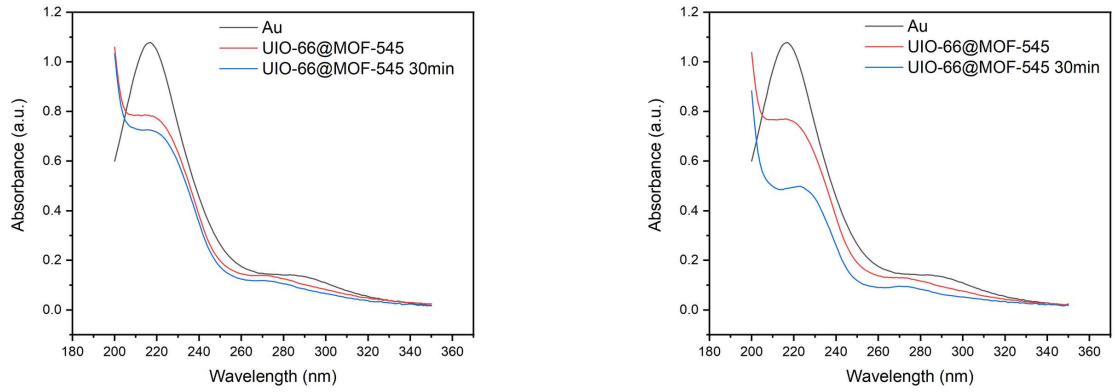


(a) The Au(III)-only control. **(b)** UIO-66

Figure 8 UV–Vis spectra showing the Au(III) concentration before and after 30 min treatment.

The Au(III)-only control showed no measurable change in absorbance between 0 and 30 min, corresponding to 0% gold removal. In comparison, UIO-66 showed a decrease in absorbance after 30 min, indicating a decrease in the Au(III) concentration remaining in solution. The calculated gold-removal efficiency was around 20% .

UIO-66@MOF-545 showed a decrease in absorbance under both conditions. The composite showed a gold-removal efficiency of 32.6% under dark conditions and 55.0% under light irradiation.



(a) Dark conditions.

(b) Light irradiation.

Figure 9 UV–Vis spectra showing the Au(III) concentration before and after 30 min for UIO-66@MOF-545.

5 Discussion

The results showed that the different MOF materials had different gold-removal efficiencies. The Au(III) control showed no change during the experimental period, providing a baseline for comparison with the MOF-containing samples. The decrease in Au(III) concentration observed for the MOF samples therefore indicates that the MOF materials contributed to the removal of gold from the aqueous solution, MOF-525 showed the highest gold removal efficiency of the individual MOFs tested, while MOF-545 also showed substantial gold removal. The difference between the two materials indicates that the structure and properties of the porphyrinic MOFs influenced their gold-removal performance [**7**]. This provides a comparison for evaluating whether combining a porphyrinic MOF with UIO-66 improved the performance of the resulting MOF-on-MOF material [**6**].

The UIO-66@MOF-545 composite showed higher gold removal under light irradiation than under dark conditions. This result is consistent with the aim of combining the structural stability of UIO-66 with the light-active properties of MOF-545 [**7**, **8**]. The higher removal under light suggests that irradiation influenced the performance of the compound [**7**]. However, the light-treated composite did not achieve the highest gold-removal efficiency observed in this study, as MOF-525 showed greater removal under the tested conditions.

The SEM results showed differences in morphology between UIO-66 and UIO-66@MOF-545, with additional surface features observed for the composite. This supported the formation of a modified surface following the growth of MOF-545 on UIO-66 [**6**]. EDS and elemental mapping were used to examine the elemental composition and distribution of the materials, while XRD was used to compare the crystalline phases of the individual MOFs and MOF-on-MOF materials. These characterization results were important for evaluating the formation of the intended heterostructure before assessing its gold-removal performance [**6**].

An unexpected result was that the UIO-66@MOF-545 compound did not show higher gold removal than MOF-525 under light irradiation. The MOF-on-MOF structure was designed to combine the properties of the two MOF components, but the results did not show an overall improvement compared with MOF-525. This indicates that combining two MOFs does not necessarily result in higher gold-removal performance and that the structure of the resulting composite can influence its performance [**6**].

UIO-66@MOF-525 could not be included in the comparison because its synthesis was not

successfully achieved. Therefore, a direct comparison between UIO-66@MOF-525 and UIO-66@MOF-545 could not be made. This limited the ability to determine whether the two porphyrinic MOFs would behave differently when incorporated into the UIO-66-based MOF-on-MOF structure.

Overall, the results show that both the MOF structure and treatment condition influenced gold recovery. The higher gold removal observed for UIO-66@MOF-545 under light compared with dark conditions supports further investigation of the composite for light-driven gold recovery [**7**, **8**]. However, further optimization is required to determine whether the MOF-on-MOF structure can provide improved gold recovery compared with the individual MOF materials [**6**].

6 Limitations and Future Work

One limitation of this study was the unsuccessful synthesis of UIO-66@MOF-525. This meant that the material could not be fully characterized or tested for gold recovery, so a direct comparison with UIO-66@MOF-545 could not be made. Future work should focus on optimizing the synthesis conditions to successfully obtain the correct UIO-66@MOF-525 structure and a uniform growth of MOF-525 on the UIO-66 surface [**6**].

Another limitation was the short treatment time and limited number of experimental repeats used for the gold-recovery experiments. Future experiments should include longer treatment times and more repeats to determine how the gold-removal efficiency changes with time and to improve the reliability of the results.

The UV–Vis analysis also only measured the change in Au(III) concentration in solution. Further analysis after gold recovery, such as EDS and elemental mapping, could be used to determine whether gold was deposited on the MOF surface and how it was distributed.

Further optimization of the MOF-on-MOF synthesis would also be useful to improve the morphology and uniformity of the materials. Different synthesis conditions and ratios of the MOF components could be tested to determine the conditions that produce the most suitable composite structure [**6**].

Future work could also investigate other applications for the newly synthesized materials. Since the materials combine porous structures with light-active properties, testing them in other applications could help identify areas where the newly synthesized MOF-on-MOF materials perform best [**9**]. This would also help determine whether their use can be extended beyond gold recovery.

7 Conclusion

This project investigated UIO-66-based MOF-on-MOF materials for light-driven gold recovery from aqueous solutions. The aim was to explore a more sustainable approach to gold recovery while supporting water sustainability and resource recovery. The materials were characterized using SEM, EDS, elemental mapping, and XRD, while UV–vis spectroscopy was used to measure the change in Au(III) concentration after treatment. MOF-525 showed the highest gold-removal efficiency at 70.33%, while MOF-545 showed 52.6% removal. UIO-66@MOF-545 showed higher gold removal under light than under dark conditions, increasing from 32.6% to 55.0%. This showed that the treatment condition affected the performance of the compound. However, UIO-66@MOF-525 was not successfully synthesized, so a direct comparison between the two MOF-on-MOF materials could not be made.

Overall, the results showed that both the MOF structure and light conditions affected gold recovery. Further work is needed to optimize the synthesis and improve the performance of the MOF-on-MOF materials. The results also show that recovering valuable metals from aqueous

waste could be useful for reducing waste and making better use of water resources [**1**, **2**, **3**]. Developing materials that can support both resource recovery and the treatment of contaminated water could contribute to more sustainable water management [**1**, **2**].

8 Acknowledgments

I would like to sincerely thank UNSW for hosting me and KAUST for providing me with this opportunity to gain research experience in a new environment. I am especially grateful to my supervisor, Dr. Kang Liang, for his guidance and support throughout this project, and to my mentor, Yanhan Wang, for his continuous help and guidance throughout the project and for always being there to support me in the lab.

I would also like to thank Jueyi Xue for her help with the laboratory work and for her support during the experimental process. I am grateful to everyone who contributed to making this experience a valuable and enjoyable learning opportunity.

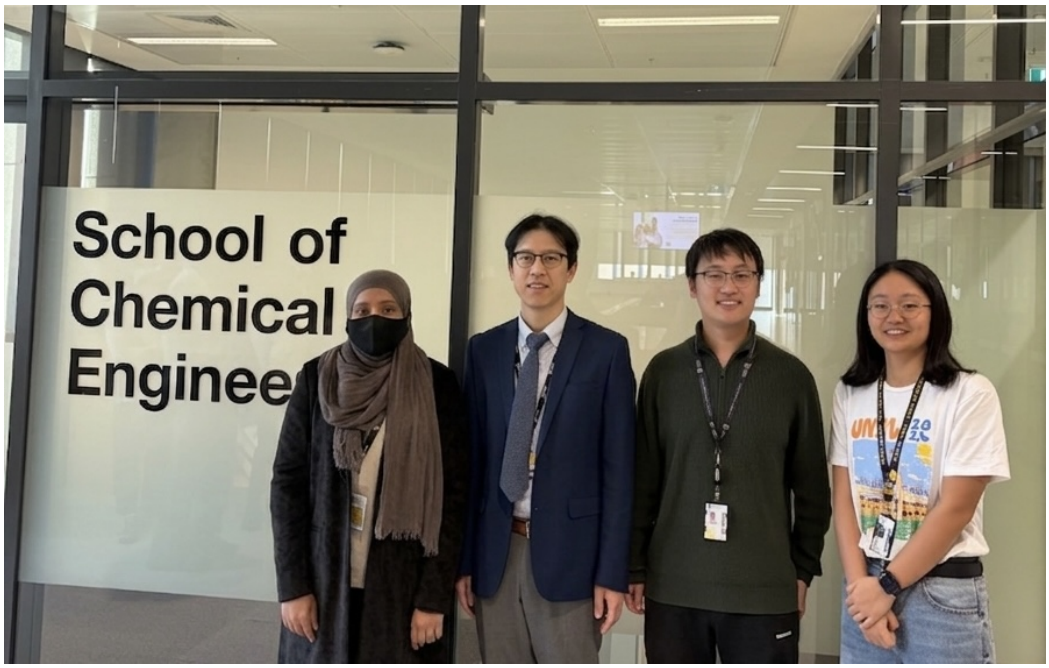


Figure 10 Research team at UNSW. From left to right: Leena Alqmize, Dr. Kang Liang, Yanhan Wang, and Jueyi Xue.

9 References

[1] UNESCO, *The United Nations World Water Development Report 2024: Water for Prosperity and Peace*. United Nations Educational, Scientific and Cultural Organization, 2024.

[2] UN-Water, *Progress on SDG 6: Clean Water and Sanitation*. United Nations, 2024.

[3] Y. Geng et al., "Towards a Circular Economy: Progress and Challenges," *Journal of Cleaner Production*, vol. 279, Art. no. 123887, 2021. doi: 10.1016/j.jclepro.2020.123887.

[4] M. K. Jha et al., "Recovery of Gold and Other Precious Metals from E-Waste: A Review," *Waste Management*, vol. 57, pp. 255–267, 2016. doi: 10.1016/j.wasman.2016.07.014.

[5] Z. Chang, F. Li, X. Qi, B. Jiang, J. Kou, and C. Sun, "Selective and Efficient Adsorption of Au(III) in Aqueous Solution by Zr-Based Metal-Organic Frameworks (MOFs): An Unconventional Way for Gold Recycling," *Journal of Hazardous Materials*, vol. 391, Art. no. 122175, 2020. doi: 10.1016/j.jhazmat.2020.122175.

[6] C. Liu, L. Lin, Q. Sun, J. Wang, R. Huang, W. Chen, S. Li, J. Wan, J. Zou, and C. Yu, "Site-Specific Growth of MOF-on-MOF Heterostructures with Controllable Nano-Architectures: Beyond the Combination of MOF Analogues," *Chemical Science*, vol. 11, no. 14, pp. 3680–3686, 2020. doi: 10.1039/D0SC00417K.

[7] Y. Shu, Y. Chen, Q. Han, X. Liu, B. Liu, and Z. Wang, "Selective and Light-Enhanced Au(III) Recovery by a Porphyrin-Based Metal-Organic Framework: Performance and Underlying Mechanisms," *ACS ES&T Engineering*, vol. 3, no. 7, pp. 1042–1052, 2023. doi: 10.1021/acsestengg.3c00082.

[8] J. Cao, Z. Xu, Y. Chen, S. Li, Y. Jiang, L. Bai, H. Yu, H. Li, and Z. Bian, "Tailoring the Asymmetric Structure of NH_2-UiO-66 Metal-Organic Frameworks for Light-Promoted Selective and Efficient Gold Extraction and Separation," *Angewandte Chemie International Edition*, vol. 62, no. 18, Art. no. e202302202, 2023. doi: 10.1002/anie.202302202.

[9] D. Lan, J. Xue, Q. Chen, P. Deng, H. Zong, Y. Chi, J. Tang, and K. Liang, "Self-Propelled MOF Nanomotors for Dual-Function Capture and Photocatalytic Removal of Organic Contaminant in Water," *Sustainable Materials and Technologies*, vol. 43, Art. no. e01324, 2025. doi: 10.1016/j.susmat.2025.e01324.